Progress In Electromagnetics Research C, Vol. 67, 185–192, 2016

An Improved Broadband SIW Phase Shifter with Embedded Air Strips

Hao Peng[1, *], Xinlin Xia[1], Serioja O. Tatu[2], and Tao Yang[1]

Abstract—In this paper, an improved broadband substrate integrated waveguide (SIW) phase shifter with embedded air strips is presented. Phase shifter can be generated based on the variable widths of SIW, variable lengths of microstrip line and a row of embedded air strips. The simulated and measured results both show that this kind of SIW phase shifter has excellent performance for a wider bandwidth. Measured results indicate that the proposed SIW phase shifters for the 45° and 90° versions have achieved the fractional bandwidths of 59.6% from 10.2 to 18.85 GHz with the accuracy of 2.5°, and of 62.3% from 9.5 to 18.1 GHz with the accuracy of 5°, respectively. The return losses are better than 15.8 dB and 14.5 dB for 45° and 90° modules, respectively. In addition, the insertion losses are both found to be better than 1.6 dB in the considered band.

1. INTRODUCTION

Phase shifter plays an extreme role in the microwave and millimeter-wave circuits and systems such as phase discriminator, phased array, instrumentation and measurement system, etc. Substrate integrated waveguide technology has several advantages such as low insertion and radiation loss, high Q-factor, easy integration with the active circuit, etc. [1]. So far, some SIW phase shifters have been studied and proposed depended with different design methods [2–4]. In [2], a self-compensating phase shifter combining delay line and equal-length unequal-width phase shifter has been designed and fabricated. Although the fractional bandwidths are close to 50%, their drawbacks are that the reference phase lines are variable for different phase shifts. In addition, the fractional bandwidth needs to be expanded due to higher demands in communication technology and instrumentation system. In [3], phase shifter, which consists of a SIW section with two inserted metallic posts, is designed. In [4] and [5], phase shifts can be controlled digitally by burying NIP diodes within the substrate at specific positions, or placing PIN diodes on the metal material structure as a load. However, the bandwidths are limited and unsatisfactory. To form a phase shifter with a 15° phase gradient, several phase channels are introduced based on the SIW resonators loaded with extra metallic posts [6]. Obviously, the phase shifter has the characteristics of narrowband and limited phase range. To reduce the size of phase shifter, a broadband compact SIW phase shifter is designed using Omega particles [7]. However, compared with simulation, the measurement results seem not to be ideal. A higher insertion loss will also limit its applications. In [8], the rod-loaded artificial dielectric slab, which uses an array of metallic rods in the middle of a SIW, is introduced to expand the bandwidth (46%) and enhance the integration. Its bandwidth should be extended for a further application. A broadband phase shifter using round air holes with different diameters in SIW is designed and manufactured [9]. It can reach a fractional bandwidth of 40.6% and a phase shift of about 40°. In addition, some SIW phase shifters are controlled by electronic tunable

Received 9 August 2016, Accepted 14 September 2016, Scheduled 27 September 2016

* Corresponding author: Hao Peng (penghao@uestc.edu.cn).

[1] School of Electronic Engineering, University of Electronic Science and Technology of China, Chengdu, Sichuan 611731, P. R. China. [2] Institut National de la Recherche Scientifique, Centre Énergie, Matériaux, Télécommunications, 800 de la Gauchetière Ouest, Montréal, QC, H5A 1K6, Canada.

voltages based on the operating state of diodes [10–12]. These phase shifters are needed to further expand bandwidth. In [13], the researchers have focused on the millimeter-wave ferrite phase shifter in substrate integrated waveguide. The model of ferrite phase shifter is discussed and illustrated. Its bandwidth is about 20% in theory. An X-band ferrite-loaded half mode SIW (HMSIW) phase shifter is presented in [14]. Its insertion loss is less than 3.2 dB at the frequency range from 9.7 to 11 GHz with the return loss of 10 dB. In addition, the phase shifters based on switched-line with loadedline [15] and the composite right/left handed transmission line (CRLH TL) [16] have been discussed. The bandwidths should be expanded for a wider application.

In this paper, an improved broadband substrate integrated waveguide phase shifter with embedded air strips is presented. The measurement results show that it can simultaneously obtain a wider bandwidth and phase accuracies comparing with previous ones.

2. CONFIGURATION AND THEORY

Figure 1 shows the configuration of the proposed broadband SIW phase shifter with embedded air strips. For the constant reference line, it seems to be the same as the new wideband SIW structure [17], which is formed by two rows of metallized vias, four metallized vias on the edge of SIW section, two microstrip-to-SIW transitions and two microstrip lines. For the phase shifters, a row of embedded air strips is additionally added to both generate phase shift and expand the bandwidth. The propagation speed of electromagnetic waves in different dielectric constants is totally different. For the several dielectric materials, the phase shift with bigger dielectric constant is more than the others on the condition of the same SIW width and length. It is noted that the phase shift mentioned above is not constant with frequency changes. So the comprehensive compensation method, based on different lengths of microstrip lines, different filled dielectric materials, and different SIW widths, is discussed then. In essential, the embedded air strip can be considered as an irregular air chamber with non-metallic side walls. To constrain electromagnetic field in SIW and avoid radiation leakage into the free space, a piece of metallized PCB cover is used.

For microstrip line, the first-order derivative of phase shift $\varphi(f)_m = \beta(f)_m \cdot \Delta l_m$ can be expressed as:

$$\frac{d\varphi\,(f)_m}{df} = \frac{2\pi\sqrt{\varepsilon_e}}{c}\,(l_{m2} - l_{m1}) \tag{1}$$

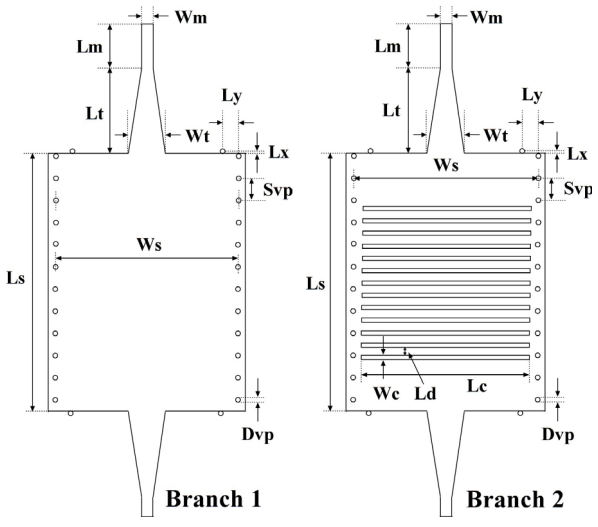

(a) (b)

Figure 1. Configuration of the proposed broadband SIW phase shifter. (a) Top view of constant reference line, (b) top view of phase shifters.

ε_e, which represents equivalent substrate permittivity for microstrip line.

For SIW sections of branch 1 and branch 2, the phase difference can be written as (f: gigahertz, W_{es1} and W_{es2}: millimeters) [2]:

$$\begin{aligned}\varphi(f)_s &= \sum_{i=1}^{n}\sqrt{\left(\frac{2\pi\sqrt{\varepsilon_0}f}{300}\right)^2-\left(\frac{\pi}{W_{es2}}\right)^2}\cdot W_{ci}+\sum_{i=1}^{m}\sqrt{\left(\frac{2\pi\sqrt{\varepsilon_r}f}{300}\right)^2-\left(\frac{\pi}{W_{es2}}\right)^2}\\ &\quad\cdot L_{di}-\sqrt{\left(\frac{2\pi\sqrt{\varepsilon_r}f}{300}\right)^2-\left(\frac{\pi}{W_{es1}}\right)^2}\cdot L_s\\ &= \sum_{i=1}^{n}\left(\sqrt{\left(\frac{2\pi\sqrt{\varepsilon_0}f}{300}\right)^2-\left(\frac{\pi}{W_{es2}}\right)^2}-\sqrt{\left(\frac{2\pi\sqrt{\varepsilon_r}f}{300}\right)^2-\left(\frac{\pi}{W_{es1}}\right)^2}\right)\\ &\quad\cdot W_{ci}+\sum_{i=1}^{m}\left(\sqrt{\left(\frac{2\pi\sqrt{\varepsilon_r}f}{300}\right)^2-\left(\frac{\pi}{W_{es2}}\right)^2}-\sqrt{\left(\frac{2\pi\sqrt{\varepsilon_r}f}{300}\right)^2-\left(\frac{\pi}{W_{es1}}\right)^2}\right)\cdot L_{di}\end{aligned}\tag{2}$$

where

$$L_s=\sum_{i=1}^{n}W_{ci}+\sum_{i=1}^{m}L_{di}$$

W_{es1} and W_{es2} are equivalent widths of SIW, which can be expressed as follows [2]:

$$W_{es}=W_s-\frac{D_{vp}^2}{S_{vp}}\tag{3}$$

The first-order derivative of phase shift $\varphi(f)_s$ has the following form:

$$\begin{aligned}\frac{d\varphi(f)_s}{df} &= \frac{4\pi\cdot f\left(\sum_{i=1}^{n}W_{ci}\right)}{300^2}\underbrace{\left(\frac{\varepsilon_0}{\sqrt{\left(\frac{2\sqrt{\varepsilon_0}f}{300}\right)^2-\left(\frac{1}{W_{es2}}\right)^2}}-\frac{\varepsilon_r}{\sqrt{\left(\frac{2\sqrt{\varepsilon_r}f}{300}\right)^2-\left(\frac{1}{W_{es1}}\right)^2}}\right)}_{Part1}\\ &\quad+\frac{4\pi\cdot\varepsilon_r\cdot f\left(\sum_{i=1}^{m}L_{di}\right)}{300^2}\underbrace{\left(\frac{1}{\sqrt{\left(\frac{2\sqrt{\varepsilon_r}f}{300}\right)^2-\left(\frac{1}{W_{es2}}\right)^2}}-\frac{1}{\sqrt{\left(\frac{2\sqrt{\varepsilon_r}f}{300}\right)^2-\left(\frac{1}{W_{es1}}\right)^2}}\right)}_{Part2}\end{aligned}\tag{4}$$

In Eq. (4), parameters m and n represent the number of air strips and number of medium strips, respectively, with $n=m+1$. For the part 2 of Eq. (4), the calculation value is less than zero under the condition $W_{es2}>W_{es1}$. But the positive and negative regions for part 1 in Eq. (4) cannot be judged from the mathematical view. In fact, it will be less than zero based on some reasonable choice for physical parameters. This conclusion will be mentioned and proved in the following content.

The microstrip length $l_{m2}>l_{m1}$ and SIW equivalent width $W_{es2}>W_{es1}$ are assumed. Eq. (1) and Eq. (4) mean that $\varphi(f)_m$ and $\varphi(f)_s$ have totally different trends. If combining two classes of phase shifters above, the sum phase can be compensated each other with frequency.

3. PHASE SHIFTER DESIGN

In this paper, all phase shifters are fabricated on an RT/Duroid 5880 substrate with a permittivity of 2.2, loss tangent of 0.0009 and thickness of 0.787 mm. The phase shifters are simulated and optimized by Ansoft HFSS.

That part 1 of Eq. (4) should be less than zero and the mathematical relationship can be established means:

$$\begin{cases} \dfrac{\varepsilon_0}{\sqrt{\left(\dfrac{2\sqrt{\varepsilon_0}f}{300}\right)^2-\left(\dfrac{1}{W_{es2}}\right)^2}} < \dfrac{\varepsilon_r}{\sqrt{\left(\dfrac{2\sqrt{\varepsilon_r}f}{300}\right)^2-\left(\dfrac{1}{W_{es1}}\right)^2}} \\ \dfrac{\sqrt{\varepsilon_0}f}{150} > \dfrac{1}{W_{es2}}, \quad \dfrac{\sqrt{\varepsilon_r}f}{150} > \dfrac{1}{W_{es1}} \end{cases} \tag{5}$$

It can be simplified as:

$$\begin{cases} \dfrac{\varepsilon_0 \cdot \varepsilon_r \cdot f^2}{150^2}(\varepsilon_0-\varepsilon_r) < \dfrac{\varepsilon_0^2}{W_{es1}^2}-\dfrac{\varepsilon_r^2}{W_{es2}^2} \\ \dfrac{\sqrt{\varepsilon_0}f}{150} > \dfrac{1}{W_{es2}}, \quad \dfrac{\sqrt{\varepsilon_r}f}{150} > \dfrac{1}{W_{es1}} \end{cases} \tag{6}$$

Parameters ε_0 and ε_r are equal to 1 and 2.2, respectively. The lower and upper frequency can be defined as 9.3 GHz and 20 GHz in this paper. So Eq. (6) can be written as:

$$\begin{cases} -0.047 < \dfrac{1}{W_{es1}^2}-\dfrac{4.84}{W_{es2}^2} \\ W_{es2} > 16.1\,\text{mm}, \quad W_{es1} > 10.75\,\text{mm} \end{cases} \tag{7}$$

The physics parameters should meet the condition of Eq. (7) in theory. Fig. 2 shows the E-field distributions of 45° and 90° phase shifters with embedded air strips at the frequency of 15 GHz. It is indicated that the transmission TE_{10} mode is very similar to the situation of traditional SIW, and the phenomenon of phase shift is excited.

Table 1 lists the dimensions of the phase shifters shown in Fig. 1. It includes the constant reference line, 45° and 90° phase shifters. Thirteen embedded air strips are introduced in the design.

Seen from Table 1, the final dimensions of phase shifters have met Eq. (7). It can be deduced that the theory in Section 2 has been verified. Based on the parameters in Table 1, the function equation

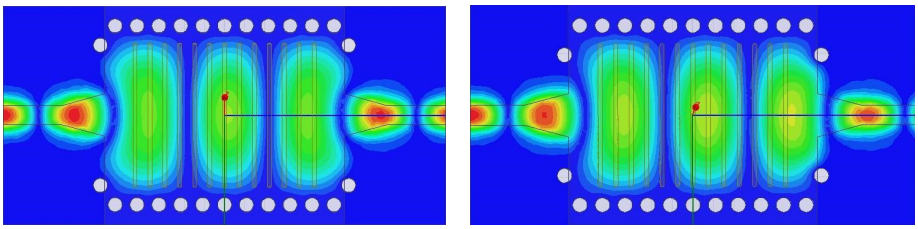

(a) (b)

Figure 2. E-field distributions of phase shifters. (a) 45° E-field distributions, (b) 90° E-field distributions.

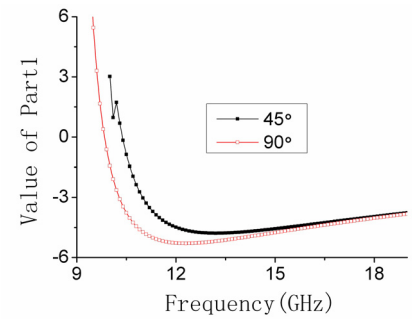

Figure 3. Calculated value of Part1 of Eq. (3).

Table 1. Dimensions of phase shifters (Unit: millimeter).

Parameters (mm)	reference line	45°	90°
Wm	1.92		
Lm	4	5.275	5.85
Lt	4.27		
Wt	4.2		
Ws	14.4	17.4	17.9
Ls	24.2		
Svp	2.2		
Dvp	1.43		
Lx	0.38		
Ly	0.85	2.85	1.95
Lc	/	13.9	14.4
Wc	/	0.4	
Ld	/	1.1	
$Wes1$ and $Wes2$	13.32	16.32	16.82

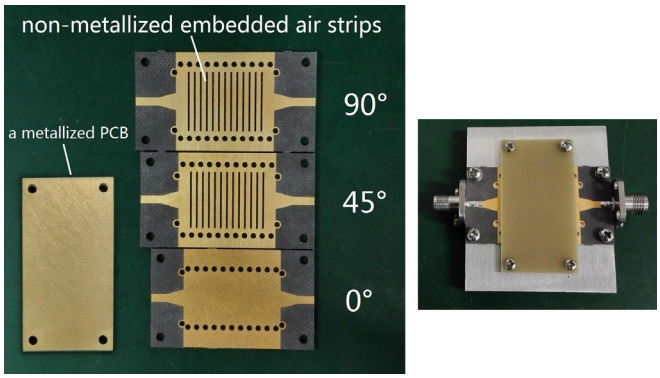

Figure 4. Fabricated and assembled phase shifters.

curve in Part 1 of Eq. (4) can be drawn in Fig. 3. In a certain range of frequency band for some reasonable choice of physical parameters, the calculation value is less than zero.

From Table 1, the main differences between phase shifters are the length of microstrip lines and width of SIW. The parameter Ly is represented as the longitudinal distance between the metallized vias on the edge of SIW section, which are mainly used to improve the input VSWR, and the row of metallized vias formed SIW section.

4. SIMULATION AND EXPERIMENT RESULTS

According to the analysis above, phase shifters with a wider bandwidth have been designed and fabricated. Shown in Fig. 4, the constant reference line, 45° and 90° phase shifters with thirteen embedded air strips are listed. The air strips formed based on hollow processing technology means that part of the copper and dielectric material are removed during processing. The air is used as filled material instead of an RT/Duroid 5880 substrate. The metallized PCB, which is perpendicular to the SIW propagation direction of electromagnetic waves, must be closely covered on the Branch 2 viewed in Fig. 4 to avoid electromagnetic radiation leakage. The gap between the metallized PCB cover and

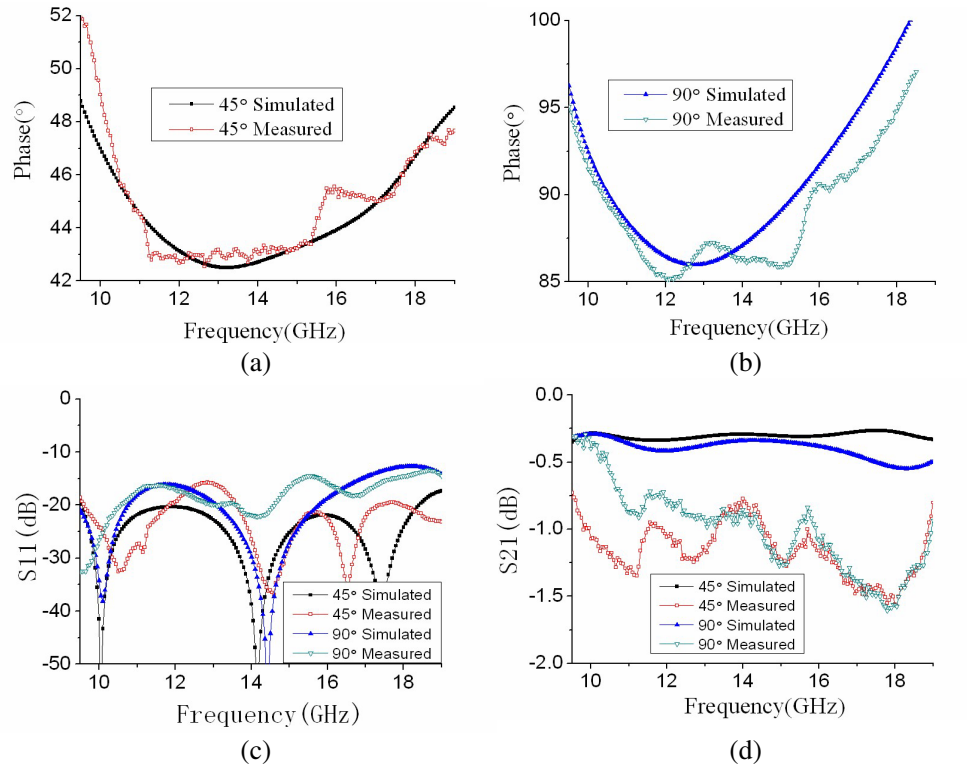

Figure 5. Simulated and measured results. (a) Phase difference for 45°, (b) phase difference for 90°, (c) S_{11}, (d) S_{21}.

Table 2. Comparison of SIW phase shifters.

	Phase shift	f (GHz)	Bandwidth	S_{11} (dB)	IL (dB)
[2]	45°±3.5°	24–40	50%	< -10.8	< 1
	90° ± 2.5°	25.11–39.75	45.1%	< -13	< 1
[7]*	45° ± 2.5°	4.487–8.355	60%	< -10	/
	90° ± 3°	4.2–7.385	55%	< -10	/
[8]	45° ± 2.5°	20–32	46%	< -12	< 0.7
	90° ± 5°	20–32	46%	< -12	< 0.7
[9]	41° ± 3.5°/40.8° ± 2.6°	26.5–40	40.6%	< -10	< 1.5
This work	45° ± 2.5°	10.2–18.85	59.6%	< -15.8	< 1.6
	90° ± 5°	9.5–18.1	62.3%	< -14.5	< 1.6

Branch 2 should be as small as possible.

A vector network analyzer (Agilent E8363B) is used to measure S-parameters. Fig. 5 shows the simulation and measurement results of phase shifters. Measured results show that the improved SIW phase shifters for 45° and 90° have achieved fractional bandwidths of 59.6% from 10.2 to 18.85 GHz with the accuracy of 2.5°, and of 62.3% from 9.5 to 18.1 GHz with the accuracy of 5°, respectively. For the measured data, the return losses are better than 15.8 dB and 14.5 dB for the 45° and 90° shifts, respectively. The insertion losses in the respective defined bandwidth are both found to be less than 1.6 dB. The differences between the simulation and measurement results may be owing to the fabrication, assembly deviations, and connectors.

Table 2 summarizes a comparison between this work and the previous published SIW phase shifters.

It can be clearly seen that a wider bandwidth and better return loss have been both obtained for this improved SIW phase shifter. Compared with [2], a wider bandwidth (about $10\% \sim 15\%$) with a similar size has been achieved. In addition, paper [7] only shows the exact simulated results' data and rough measured results' figures. Its measured insertion loss (about -5 dB) is seen to be unsatisfactory for its applications. This kind of phase shifter can be applied in six-port junction to replace the 90° microstrip line phase shifter, whose main disadvantage is the narrow bandwidth (about only 10% relative bandwidth for $90^\circ \pm 5^\circ$) [18, 19].

5. CONCLUSION

An improved broadband SIW phase shifter with embedded air strips is presented in this paper. A row of air strips are introduced into the design to expand the bandwidth. Four metallized vias are added to improve the input VSWR. The measured results show a good agreement with the simulated ones. With an excellent performance of bandwidth, a better return loss and an acceptable insertion loss have been achieved.

ACKNOWLEDGMENT

The authors gratefully acknowledge financial support from China Scholarship Council (CSC). This work was supported by the China Postdoctoral Science Foundation under Grant 2014M552337.

REFERENCES

1. Cassivi, Y., L. Perregrini, P. Arcioni, M. Bressan, K. Wu, and G. Conciauro, "Dispersion characteristics of substrate integrated rectangular waveguide," *IEEE Microwave Wireless Components Letters*, Vol. 12, No. 9, 333–335, Sep. 2002.
2. Cheng, Y. J., W. Hong, and K. Wu, "Broadband self-compensating phase shifter combining delay line and equal-length unequal-width phaser," *IEEE Transactions on Microwave Theory and Technology*, Vol. 58, No. 1, 203–210, Jan. 2010.
3. Sellal, K., L. Talbi, T. A. Denidni, and J. Lebel, "Design and implementation of a substrate integrated waveguide phase shifter," *IET Microwaves Antennas and Propagation*, Vol. 2, No. 2, 194–199, Mar. 2008.
4. Sellal, K., L. Talbi, and M. Nedil, "Design and implementation of a controllable phase shifter using substrate integrated waveguide," *IET Microwaves Antennas and Propagation*, Vol. 6, No. 9, 1090–1094, Jun. 2012.
5. Kuhestani, H., M. Naser-Moghadasi, M. Maleki, and F. B. Zarrabi, "Phase shifter designing base on half mode substrate integrated waveguide with reconfigurable quality," *Microwave and Optic Technology Letters*, Vol. 57, No. 11, 2562–2567, Aug. 2015.
6. Yang, T., M. Ettorre, and R. Sauleau, "Novel phase shifter design based on substrate-integrated-waveguide technology," *IEEE Microwave Wireless Components Letters*, Vol. 22, No. 10, 518–520, Oct. 2012.
7. Ebrahimpouri, M., S. Nikmehr, and A. Pourziad, "Broadband compact SIW phase shifter using Omega particles," *IEEE Microwave Wireless Components Letters*, Vol. 24, No. 11, 748–750, Nov. 2014.
8. Djerafi, T., K. Wu, and S. O. Tatu, "Substrate-integrated waveguide phase shifter with rod-loaded artificial dielectric slab," *Electronics Letters*, Vol. 51, No. 9, 707–709, Apr. 2015.
9. Boudreau, I., K. Wu, and D. Deslandes, "Broadband phase shifter using air holes in substrate integrated waveguide," *IEEE MTT-S International Microwave Symposium Digest*, 1–4, Baltimore, United States, 2011.
10. Yang, F., H. X. Yu, B. Zhang, Y. Zhou, and Z. X. Zhu, "Substrate integrated waveguide phase shifter," *International Conference on Electronics, Communications and Control*, 3966–3968, Zhejiang, China, 2011.

11. Ding, Y. and K. Wu, "SIW varactor-tuned phase shifter and phase modulator," *IEEE MTT-S Int. Microwave Symposium Digest*, 1–3, Montreal, Canada, 2012.
12. Ding, Y. and K. Wu, "Varactor-tuned substrate integrated waveguide phase shifter," *IEEE MTT-S Int. Microwave Symposium Digest*, 1-4, Baltimore, United States, 2011.
13. Che, W., E. K.-N. Yung, K. Wu, and X. Nie, "Design investigation on millimeter-wave ferrite phase shifter in substrate integrated waveguide," *Progress In Electromagnetics Research*, Vol. 45, 263–275, 2004.
14. Cheng, Y. J., Q. Huang, Y. Zhou, and C. Weng, "Ferrite-loaded half mode substrate integrated waveguide phase shifter," *Progress In Electromagnetics Research Letters*, Vol. 47, 85–90, 2014.
15. Wang, Z., B. Yan, R.-M. Xu, and Y. Guo, "Design of a ku band six bit phase shifter using periodically loaded-line and switched-line with loaded-line," *Progress In Electromagnetics Research*, Vol. 76, 369-379, 2007.
16. Cao, W.-Q., B. Zhang, A. Liu, T. Yu, D. Guo, and Y. Wei, "Novel phase-shifting characteristic of CRLH TL and its application in the design of dual-band dual-mode dual-polarization antenna," *Progress In Electromagnetics Research*, Vol. 131, 375–390, 2012.
17. Kordiboroujeni, Z. and J. Bornemann, "New wideband transition from microstrip line to substrate integrated waveguide," *IEEE Transactions on Microwave Theory and Technology*, Vol. 62, No. 12, 2983–2989, Dec. 2014.
18. Bosisio, R. G., Y. Y. Zhao, X. Y. Xu, S. Abielmona, E. Moldovan, Y. S. Xu, M. Bozzi, S. O. Tatu, C. Nerguisian, J. F. Frigon, C. Caloz, and K. Wu, "New-wave radio," *IEEE Microwave Magazine*, Vol. 9, No. 1, 89–100, Feb. 2008.
19. Boukari, B., E. Moldovan, R. I. Cojocaru, K. Wu, R. G. Bosisio, and S. O. Tatu, "Millimeter-wave six-port in combined microstrip and substrate-integrated waveguide technologies," *Microwave and Optic Technology Letters*, Vol. 52, No. 11, 2488–2493, Aug. 2010.